

Computing the Heat of Adsorption using Molecular Simulations: The Effect of Strong Coulombic Interactions

T. J. H. Vlugt,^{*,†} E. García-Pérez,[‡] D. Dubbeldam,[§] S. Ban,^{||} and S. Calero[‡]

Process & Energy Laboratory, Delft University of Technology, Leeghwaterstraat 44, 2628CA Delft, The Netherlands, Department of Physical, Chemical, and Natural Systems, University Pablo de Olavide, Ctra. Utrera km 1, 41013 Sevilla, Spain, Chemical and Biological Engineering Department, Northwestern University, 2145 Sheridan Road, Evanston, Illinois 60208, and Condensed Matter and Interfaces, Utrecht University, P.O. Box 80000, 08 TA Utrecht, The Netherlands

Received December 18, 2007

Abstract: Molecular simulations are an important tool for the study of adsorption of hydrocarbons in nanoporous materials such as zeolites. The heat of adsorption is an important thermodynamic quantity that can be measured both in experiments and molecular simulations, and therefore it is often used to investigate the quality of a force field for a certain guest–host (*g* - *h*) system. In molecular simulations, the heat of adsorption in zeolites is often computed using either of the following methods: (1) using the Clausius-Clapeyron equation, which requires the partial derivative of the pressure with respect to temperature at constant loading, (2) using the energy difference between the host with and without a single guest molecule present, and (3) from energy/particle fluctuations in the grand-canonical ensemble. To calculate the heat of adsorption from experiments (besides direct calorimetry), only the first method is usually applicable. Although the computation of the heat of adsorption is straightforward for all-silica zeolites, severe difficulties arise when applying the conventional methods to systems with nonframework cations present. The reason for this is that these nonframework cations have very strong Coulombic interactions with the zeolite. We will present an alternative method based on biased interactions of guest molecules that suffers less from these difficulties. This method requires only a single simulation of the host structure. In addition, we will review some of the other important issues concerning the handling of these strong Coulombic interactions in simulating the adsorption of guest molecules. It turns out that the recently proposed Wolf method (*J. Chem. Phys.* **1999**, *110*, 8254) performs poorly for zeolites as a large cutoff radius is needed for convergence.

1. Introduction

Zeolites are microporous crystalline materials with pores of about the same size of a small molecule like water or n-hexane. The structure of a zeolite consists of covalently

bonded TO₄ units, in which the T-atom is usually a silicon (Si) or an aluminum (Al) atom. To obey charge neutrality, the substitution of a silicon atom by an aluminum atom requires the presence of a nonframework cation (usually Na⁺ or K⁺) or a proton (H⁺). There are approximately 170 different zeolite framework types that have been synthesized.¹ Zeolitic materials are widely used as water softener, selective adsorber, and catalyst for hydrocarbon conversions (catalytic cracking and isomerization).

* Corresponding author e-mail: t.j.h.vlugt@tudelft.nl.

[†] Delft University of Technology.

[‡] University Pablo de Olavide.

[§] Northwestern University.

^{||} Utrecht University.

As molecular simulations can provide a fundamental understanding of processes and properties at the molecular scale, in the past few years this type of simulations has become an important tool for investigating the adsorption properties of small guest (*g*) molecules in zeolite hosts (*h*). As guest–host interactions are often dominated by the dispersive interactions of the oxygen atoms with the guest,² classical force fields based on Lennard-Jones (LJ) interactions have become very popular in this field of research.^{3–10} Recently, it has been shown that an optimal parametrization can lead to united atom force fields for alkanes that are transferable to many all-silica zeolite framework types.^{11–13} This transferability is often tested by a comparison between simulations and experimental adsorption data that had not been used to calibrate the force field parameters.¹³

When nonframework cations are present in the framework, strong electrostatic interactions between the nonframework cations and the framework atoms (Si, Al, O) have to be included for a correct description of the system. Although the Ewald summation with tin foil boundary conditions is often used,¹⁴ the so-called Wolf method has been introduced recently as a pairwise alternative.^{15,16} The strong interaction between the nonframework cations and hydrocarbons lead to an enormous effect on adsorption properties.^{17–20}

In this work, we will consider the effect of strong electrostatic interactions between the framework and the nonframework cations or adsorbates on the computation of the heat of adsorption. This quantity describes the change in enthalpy when a molecule is transferred from the gas phase into the pores of a zeolite. In experiments, the heat of adsorption is usually computed using the Clausius-Clapeyron equation²¹ or direct calorimetry experiments²² while in molecular simulations this quantity is usually calculated directly from the total energy of the simulated system.^{4,23,8} However, we will show that a direct computation using energy differences results in very inaccurate results for zeolites with strongly bound nonframework cations.

This paper is organized as follows. In section 2 we briefly review the various schemes to compute the heat of adsorption in molecular simulations, and we will explain the advantages and disadvantages of each method. In particular, we will show that a direct calculation of the heat of adsorption using energy differences may lead to problems for systems with strongly interacting nonframework cations. We will introduce an alternative method based on biased insertions that does not suffer from these difficulties. Results of the various methods for a typical system (described in section 3) are presented in section 4. In section 5 we discuss some of the other important issues for handling the Coulombic interactions in these systems and show why the Ewald summation is here preferable over the recently proposed Wolf method. Our findings are summarized in section 6.

2. Calculating the Heat of Adsorption

In the remainder of this paper, we will denote the zeolite and the included nonframework cations as the “host” (*h*). The scaled positions of all the atoms that belong to the host are denoted by the vector **h**. The adsorbate is denoted as “guest” (*g*), and its conformation is denoted by **g**. In most of the derivations in this work, the heat of adsorption is calculated in molecular units, i.e. in J (or kJ) per molecule instead of the often used J per mol.

Following Wood, Panagiotopoulos, and Rowlinson,²¹ the heat of adsorption *q* (or enthalpy of adsorption - ΔH) at loading θ is defined using the famous Clausius-Clapeyron equation

$$-q = \Delta H = k_B \left(\frac{\partial \ln[P/P_0]}{\partial T^{-1}} \right)_{\theta=\text{constant}} = \left(\frac{\partial \ln[P/P_0]}{\partial \beta} \right)_{\theta=\text{constant}} \quad (1)$$

where *P* is the pressure, *P*₀ is an arbitrary reference pressure, *T* is the absolute temperature, θ is the loading of guest molecules, $k_B = R/N_{\text{av}}$ is the Boltzmann constant, *R* is the gas constant, *N*_{av} is Avogadro’s number, and $\beta = 1/(k_B T)$. For an in-depth review of the thermodynamic definition of the heat of adsorption we refer the reader to ref 24. To compute the heat of adsorption at loading θ directly from this equation, one needs the adsorption isotherm $\theta(P)$ for various temperatures *T*. At sufficiently low loadings, the gas phase will behave as an ideal gas, and the adsorption isotherm will become a linear function

$$K_H = \frac{\theta}{VP} \quad (2)$$

in which *V* is the volume of the host, and *K*_H is the so-called Henry coefficient (in units of molecules per unit of host volume per unit of pressure). The heat of adsorption at low loading then becomes

$$-q = \Delta H = - \frac{\partial \ln[K_H/K_{H0}]}{\partial \beta} \quad (3)$$

in which *K*_{H0} is an arbitrary constant (that has the same units as *K*_H). In molecular simulations, the most convenient way to calculate the Henry coefficient is using Widom’s test particle method^{14,25–27}

$$K_H = \beta \times \exp[-\beta \mu_{\text{ex}}] = \beta \times \frac{\langle \exp[-\beta u^+] \rangle_H}{\langle \exp[-\beta u_{\text{IG}}^+] \rangle_{\text{EB}}} \quad (4)$$

in which μ_{ex} is the excess chemical potential of the guest in the zeolite, u^+ is the energy of a test (guest) molecule inserted at a random position in the zeolite, and u_{IG}^+ is the energy of a test (guest) molecule inserted at a random position in an empty box without the presence of the host (often referred to as an isolated chain). The brackets $\langle \dots \rangle_H$ denote an average in the NVT ensemble over all conformations of the host (and positions of the test particle), and the brackets $\langle \dots \rangle_{\text{EB}}$ denote an ensemble average for a test chain in an empty simulation box (ideal gas phase). For chain molecules like alkanes, it is well-known that insertion of a test chain at a random position in the zeolite nearly always results in overlaps with zeolite atoms, and

therefore the sampling statistics of the average $\langle \exp[-\beta u^+] \rangle_H$ will be extremely poor.²³ For chains that are not too long (< 50 monomers) it is convenient to use the Configurational-bias Monte Carlo (CBMC) method^{28–31,14} to insert test chains. In this case, the Henry coefficient is computed from²³

$$K_H = \beta \times \frac{\langle W \rangle_H}{\langle W_{IG} \rangle_{EB}} \quad (5)$$

in which $\langle W \rangle_H$ is the average Rosenbluth weight of a test chain in the host, and $\langle W_{IG} \rangle_{EB}$ is the average Rosenbluth weight of an isolated test chain in an empty box.

Calculating the heat of adsorption at low loading directly using either eq 1 or eqs 3 and 4 requires several simulations or adsorption experiments at different temperatures, and the final answer must be computed by a numerical differentiation with respect to $1/T$. As the accuracy of such a numerical differentiation strongly depends on the accuracy of the individual simulations,³² many long simulations are required to obtain an accurate value for the heat of adsorption. Therefore, two alternative methods to compute the heat of adsorption are often used in molecular simulations.

(1) From energy differences computed in the canonical (NVT) ensemble^{21,23}

$$-q = \Delta H = \langle U_1 \rangle_1 - \langle U_0 \rangle_0 - \langle U_g \rangle - \frac{1}{\beta} \quad (6)$$

in which U_N is the total energy of a host with N guest molecules present, $\langle \dots \rangle_X$ refers to an ensemble average at constant V , T , and X guest molecules, and $\langle U_g \rangle$ is the average energy of an isolated guest molecule (without the host present). The average $\langle U_g \rangle$ for a certain guest molecule only depends on temperature and needs to be calculated only once. Later, we will see that for zeolites with nonframework cations, the difference $|\langle U_1 \rangle_1 - \langle U_0 \rangle_0|$ is very small compared to either $\langle U_0 \rangle_0$ or $\langle U_1 \rangle_1$. Therefore, a direct computation of both $\langle U_0 \rangle_0$ and $\langle U_1 \rangle_1$ can lead to a very inaccurate estimate of ΔH . Note that eq 6 only applies to the heat of adsorption at zero coverage and that it assumes ideal gas behavior.

(2) From energy/particle fluctuations in the grand-canonical (μVT) ensemble,²⁴ we can approximate the change in potential energy upon adsorption of a single guest molecule²⁴

$$\langle U_{N+1} \rangle_{N+1} - \langle U_N \rangle_N \approx \left(\frac{\partial \langle U \rangle_\mu}{\partial \langle N \rangle_\mu} \right)_\beta = \left(\frac{2 \langle U \rangle_\mu}{2 \langle N \rangle_\mu} \right)_\beta = \frac{\langle U \times N \rangle_\mu - \langle U \rangle_\mu \langle N \rangle_\mu}{\langle N^2 \rangle_\mu - \langle N \rangle_\mu \langle N \rangle_\mu} \quad (7)$$

where the brackets $\langle \dots \rangle_\mu$ denote an average in the grand-canonical ensemble, N is the number of guest molecules, and μ is the chemical potential of the guest molecules. This leads to²⁴

$$-q = \Delta H = \frac{\langle U \times N \rangle_\mu - \langle U \rangle_\mu \langle N \rangle_\mu}{\langle N^2 \rangle_\mu - \langle N \rangle_\mu \langle N \rangle_\mu} - \langle U_g \rangle - \frac{1}{\beta} \quad (8)$$

ΔH in eq 8 is usually defined as the *isosteric heat of adsorption*, and it is often applied at nonzero loading.²⁴ Again, it is assumed here that the gas phase is ideal. The

disadvantage of using this method in practice is that it relies on many particle insertions and removals in the grand-canonical ensemble. The fraction of accepted trial moves in grand-canonical simulations however can be quite low, even if advanced insertion techniques are used.^{33–35} In practice, long simulations in the grand-canonical ensemble are needed to obtain accurate statistics for the averages in eq 7, especially in the limit of low chemical potential where the number of guest molecules is either 0 or 1. Therefore, we will not consider the direct use of eq 8 in the remainder of this manuscript.

It is instructive to show that eqs 3 and 6 should give the same value for ΔH at low loading. Our starting point is the observation that the Henry coefficient is related to the free energy of a guest molecule inside the host (eq 4). We will make use of the fact that partial derivatives of free energies can always be expressed as ensemble averages.¹⁴ Consider the partial derivative

$$\frac{\partial \ln \langle \exp[-\beta u^+] \rangle_H}{\partial \beta} \quad (9)$$

and denote the scaled coordinates of the host (nonframework cations included) by \mathbf{h} and the scaled coordinates of the guest molecules by \mathbf{g} . $U_0(\mathbf{h})$ is the energy of the host and $u^+(\mathbf{g}, \mathbf{h}) = U_1(\mathbf{g}, \mathbf{h}) - U_0(\mathbf{h})$ is the energy of a single guest molecule adsorbed in the host. For the canonical partition function of the host (without the guest) we can write

$$Q_0 = Q_{\text{zeolite without guest}} = \int d\mathbf{h} \exp[-\beta U_0(\mathbf{h})] \quad (10)$$

in which we have omitted the constant prefactor of the partition function.¹⁴ For the zeolite with a single guest molecule we can write

$$Q_1 = Q_{\text{zeolite with single guest molecule}} = \int d\mathbf{h} \int d\mathbf{g} \exp[-\beta(U_0(\mathbf{h}) + u^+(\mathbf{g}, \mathbf{h}))] \quad (11)$$

In this equation we separated the total energy of a zeolite with a single guest molecule into two contributions: the zeolite and the test particle. The ensemble average $\langle \exp[-\beta u^+] \rangle_H$ is therefore

$$\begin{aligned} \langle \exp[-\beta u^+] \rangle_H &= \frac{\int d\mathbf{h} \int d\mathbf{g} \exp[-\beta(U_0(\mathbf{h}) + u^+(\mathbf{g}, \mathbf{h}))]}{\int d\mathbf{h} \exp[-\beta U_0(\mathbf{h})]} \\ &= \frac{\int d\mathbf{h} [\exp[-\beta U_0(\mathbf{h})] \int d\mathbf{g} \exp[-\beta u^+(\mathbf{g}, \mathbf{h})]]}{\int d\mathbf{h} \exp[-\beta U_0(\mathbf{h})]} \end{aligned} \quad (12)$$

Taking the partial derivative of its logarithm with respect to β we get

$$\begin{aligned}
& \frac{\partial \ln \langle \exp[-\beta u^+] \rangle_{\text{H}}}{\partial \beta} \\
&= \frac{\partial}{\partial \beta} \left[\ln \left(\frac{\int d\mathbf{h} [\exp[-\beta U_0(\mathbf{h})] \int d\mathbf{g} \exp[-\beta u^+(\mathbf{g}, \mathbf{h})]]}{\int d\mathbf{h} \exp[-\beta U_0(\mathbf{h})]} \right) \right] \\
&= \frac{\int d\mathbf{h} \exp[\beta U_0(\mathbf{h})]}{\int d\mathbf{h} [\exp[-\beta U_0(\mathbf{h})] \int d\mathbf{g} \exp[-\beta u^+(\mathbf{g}, \mathbf{h})]]} \times \\
& \quad \frac{\int d\mathbf{h} \exp[-\beta U_0(\mathbf{h})] \times \int d\mathbf{h} \int d\mathbf{g} \exp[-\beta (U_0(\mathbf{h}) + u^+(\mathbf{g}, \mathbf{h}))] (-U_0(\mathbf{h}) - u^+(\mathbf{g}, \mathbf{h}))}{(\int d\mathbf{h} \exp[-\beta U_0(\mathbf{h})])^2} \\
& \quad - \frac{\int d\mathbf{h} \exp[-\beta U_0(\mathbf{h})]}{\int d\mathbf{h} [\exp[-\beta U_0(\mathbf{h})] \int d\mathbf{g} \exp[-\beta u^+(\mathbf{g}, \mathbf{h})]]} \times \\
& \quad \frac{\int d\mathbf{h} \exp[-\beta U_0(\mathbf{h})] (-U_0(\mathbf{h})) \times \int d\mathbf{h} \int d\mathbf{g} \exp[-\beta (U_0(\mathbf{h}) + u^+(\mathbf{g}, \mathbf{h}))]}{(\int d\mathbf{h} \exp[-\beta U_0(\mathbf{h})])^2} \\
&= - \frac{\int d\mathbf{h} \int d\mathbf{g} \exp[-\beta (U_0(\mathbf{h}) + u^+(\mathbf{g}, \mathbf{h}))] (U_0(\mathbf{h}) + u^+(\mathbf{g}, \mathbf{h}))}{\int d\mathbf{h} \int d\mathbf{g} \exp[-\beta (U_0(\mathbf{h}) + u^+(\mathbf{g}, \mathbf{h}))]} \\
& \quad + \frac{\int d\mathbf{h} \exp[-\beta U_0(\mathbf{h})] U_0(\mathbf{h})}{\int d\mathbf{h} \exp[-\beta U_0(\mathbf{h})]} \\
&= \langle U_0 \rangle_0 - \langle U_0 + u^+ \rangle_1 \\
&= \langle U_0 \rangle_0 - \langle U_1 \rangle_1
\end{aligned} \tag{13}$$

The same can be derived for the other term in eq 6 (corresponding to the isolated chain)

$$\begin{aligned}
& \frac{\partial \ln \langle \exp[-\beta u_{\text{IG}}^+] \rangle_{\text{EB}}}{\partial \beta} \\
&= \langle U_{\text{IG}} \rangle_{\text{empty box no chain}} - \langle U_{\text{IG}} + u_{\text{IG}}^+ \rangle_{\text{empty box with single chain}} \\
&= -\langle u_{\text{IG}}^+ \rangle_{\text{empty box with single chain}} \\
&= -\langle U_{\text{g}} \rangle
\end{aligned} \tag{14}$$

in which U_{IG} is the energy of an empty box (zero) and u_{IG}^+ is the energy of an isolated chain in this empty box. From eqs 3 and 4, we obtain

$$\begin{aligned}
\Delta H &= -\frac{\partial \ln K_{\text{H}}}{\partial \beta} = \\
& \quad -\frac{\partial}{\partial \beta} [\ln \beta + \ln \langle \exp[-\beta u^+] \rangle_{\text{H}} - \ln \langle \exp[-\beta u_{\text{IG}}^+] \rangle_{\text{EB}}] \tag{15}
\end{aligned}$$

and by substituting eqs 13 and 14 we end up with eq 6. This means that eqs 3 and 6 should give identical result for ΔH at low loading.

In this work, we propose to use eq 8 in such a way that $\langle U_{N+1} \rangle_{N+1}$ and $\langle U_N \rangle_N$ are computed in a single simulation in the NVT ensemble. This means that for the calculation of ΔH at a certain loading (N guest molecules present in the system), only a single simulation of the host structure is needed. This simulation is performed in the ensemble with N guest molecules present (denoted as $\langle \cdots \rangle_N$). Our starting point is

$$\begin{aligned}
& \langle U_{N+1} \rangle_{N+1} - \langle U_N \rangle_N \\
&= \langle U_N + u^+ \rangle_{N+1} - \langle U_N \rangle_N \\
&= \frac{\int d\mathbf{h} \int d\mathbf{g} \exp[-\beta (U_N(\mathbf{g}, \mathbf{h}) + u^+(\mathbf{g}, \mathbf{h}))] (U_N(\mathbf{g}, \mathbf{h}) + u^+(\mathbf{g}, \mathbf{h}))}{\int d\mathbf{h} \int d\mathbf{g} \exp[-\beta (U_N(\mathbf{g}, \mathbf{h}) + u^+(\mathbf{g}, \mathbf{h}))]} - \langle U_N \rangle_N \\
& \quad \frac{\int d\mathbf{h} \int d\mathbf{g} \exp[-\beta (U_N(\mathbf{g}, \mathbf{h}) + u^+(\mathbf{g}, \mathbf{h}))] (U_N(\mathbf{g}, \mathbf{h}) + u^+(\mathbf{g}, \mathbf{h}))}{\int d\mathbf{h} \int d\mathbf{g} \exp[-\beta (U_N(\mathbf{g}, \mathbf{h}) + u^+(\mathbf{g}, \mathbf{h}))]} - \langle U_N \rangle_N \\
&= -\frac{\int d\mathbf{h} \int d\mathbf{g} \exp[-\beta U_N(\mathbf{g}, \mathbf{h})]}{\int d\mathbf{h} \int d\mathbf{g} \exp[-\beta (U_N(\mathbf{g}, \mathbf{h}) + u^+(\mathbf{g}, \mathbf{h}))]} - \langle U_N \rangle_N \\
& \quad \frac{\int d\mathbf{h} \int d\mathbf{g} \exp[-\beta U_N(\mathbf{g}, \mathbf{h})]}{\int d\mathbf{h} \int d\mathbf{g} \exp[-\beta (U_N(\mathbf{g}, \mathbf{h}) + u^+(\mathbf{g}, \mathbf{h}))]} \\
&= \frac{\langle (U_N + u^+) \exp[-\beta u^+] \rangle_N - \langle U_N \rangle_N}{\langle \exp[-\beta u^+] \rangle_N} - \langle U_N \rangle_N
\end{aligned} \tag{16}$$

in which $u^+ = U_{N+1} - U_N$ is the energy of a test (guest) chain. Note that the coordinates of the test chain are included in \mathbf{h} . For chain molecules, it is much more convenient to use the Rosenbluth algorithm³⁶ to generate a conformation of a test chain. In this case, it is trivial to show that

$$\langle \exp[-\beta u^+] \rangle_N = \langle W \rangle_N \tag{17}$$

$$\langle (U_N + u^+) \times \exp[-\beta u^+] \rangle_N = \langle (U_N + u^+) \times W \rangle_N \tag{18}$$

and therefore

$$\langle U_{N+1} \rangle_{N+1} - \langle U_N \rangle_N = \frac{\langle (U_N + u^+) \times W \rangle_N}{\langle W \rangle_N} - \langle U_N \rangle_N \tag{19}$$

In the Rosenbluth algorithm, it is often convenient to use only part of the nonbonded energy to select trial segments leading to a modified Rosenbluth weight $\langle W^* \rangle$. In the Appendix, it is derived that

$$\langle W \rangle_N = \langle W^* \exp[-\beta\delta] \rangle_N \quad (20)$$

$$\langle (U_N + u^+) \times W \rangle_N = \langle (U_N + u^+) \times W^* \exp[-\beta\delta] \rangle_N \quad (21)$$

in which δ is the energy difference between the total nonbonded part of the potential and the nonbonded part of the potential that was used to select trial segments.^{27,37} The final expression then becomes

$$-q = \Delta H = \frac{\langle (U_N + u^+) \times W^* \exp[-\beta\delta] \rangle_N}{\langle W^* \exp[-\beta\delta] \rangle_N} - \langle U_N \rangle_N - \langle U_g \rangle - \frac{1}{\beta} \quad (22)$$

The ensemble averages $\langle \dots \rangle_N$ can be computed from the same simulation. Calculating $\langle U_g \rangle$ requires a simulation of an isolated guest molecule at the same temperature. It is important to note that eqs 20 and 8 lead to identical results and both can be applied at nonzero loading (in contrast to eqs 3, 4, and 5). At low loading ($N = 0$), eq 22 becomes identical to eqs 3 and 6 and not only the heat of adsorption but also the Henry coefficient can be computed using a single simulation of the host structure (this in contrast to the conventional test particle method).

In principle, one could also perform simulations in the ensemble $\langle \dots \rangle_N$ to compute averages in the ensemble $\langle \dots \rangle_{N-1}$. This leads to

$$\langle U_{N-1} \rangle_{N-1} = \frac{\langle U_{N-1} \times \exp[\beta u^+] \rangle_N}{\langle \exp[\beta u^+] \rangle_N} \quad (23)$$

with $u^+ = U_N - U_{N-1}$. This would correspond to a real-particle version of eq 16. However, as this is equivalent to computing the chemical potential using a real particle formulation, this approach will be extremely inefficient.¹⁴

3. Model and Simulation Details

To test the different methods to compute the heat of adsorption, we studied the adsorption of n-alkanes in zeolite LTA5A using the force field of ref 18. We simulated a single unit cell with dimensions of $a = b = c = 24.555 \text{ \AA}$ ($\alpha = \beta = \gamma = 90^\circ$) and with composition $\text{Na}_{32}\text{Ca}_{32}\text{Al}_{96}\text{Si}_{96}\text{O}_{384}$. Periodic boundary conditions are used. The unit cell of LTA consists of 8 cages that are interconnected by small windows, see Figure 1. The crystallographic positions of the framework atoms (Al, Si, O) as well as the initial positions of the nonframework cations (Na, Ca) are taken from the work of Pluth et al.³⁸ Electrostatic interactions are handled using the Ewald summation with parameters $\alpha = 0.3 \text{ \AA}^{-1}$ and $k = 9$ wave vectors in each reciprocal direction.¹⁴

Simulations were performed in the NVT ensemble at 500 K. In each Monte Carlo cycle, it is chosen at random with a fixed probability to displace, rotate, or regrow a hydrocarbon chain (if present in the system) at a random position.

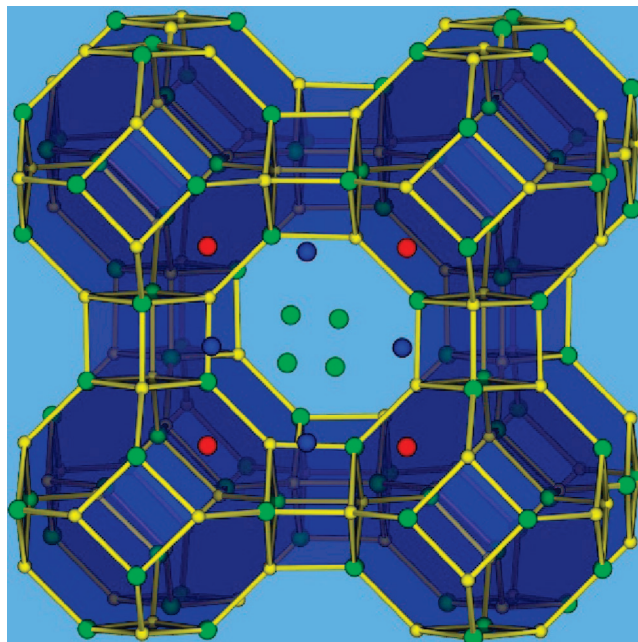


Figure 1. Schematic representation of framework type LTA.

As it is well-known that fixing the positions of the non-framework cations (Na, Ca) may lead to erroneous results,¹⁷ trial moves to displace the nonframework cations are included. The number of trial moves in each cycle is equal to the number of nonframework cations. The positions of the framework atoms (Si, Al, O) are kept fixed. During the simulations, test chains are grown using the Rosenbluth algorithm from which data on the average Rosenbluth weight of the sorbate are collected; this is used to compute the heat of adsorption using eq 22. The number of test insertions per cycle is equal to the number of nonframework cations. In this way, the amount of CPU time per cycle is approximately equal for the methods to compute the heat of adsorption (eqs 6 and 22).

4. Results

In Figure 2, we have plotted the heat of adsorption of various n-alkanes at zero loading computed using various methods. Clearly, the new method (eq 22) produces exactly the same result as the method using the temperature derivative of the Henry coefficient (eqs 3 and 4) as well as with the method based on energy differences (eq 6) within the accuracy of the simulations.

In Figure 3 we have plotted the running average of the heat of adsorption of n-hexane as a function of the number of MC cycles when small displacements of the nonframework cations are allowed. Here, the initial positions of the nonframework cations were taken from the crystallographic positions. The method based on energy differences requires two simulations of the zeolite, one with a single n-hexane chain and one without, while our new method requires only a single simulation of the host system. It turns out that each MC cycle takes approximately the same amount of CPU time for each method, and therefore it becomes clear from Figure 3 that our new method converges much more quickly to the final answer. As the difference $|\langle U_1 \rangle_1 - \langle U_0 \rangle_0|$ is typically

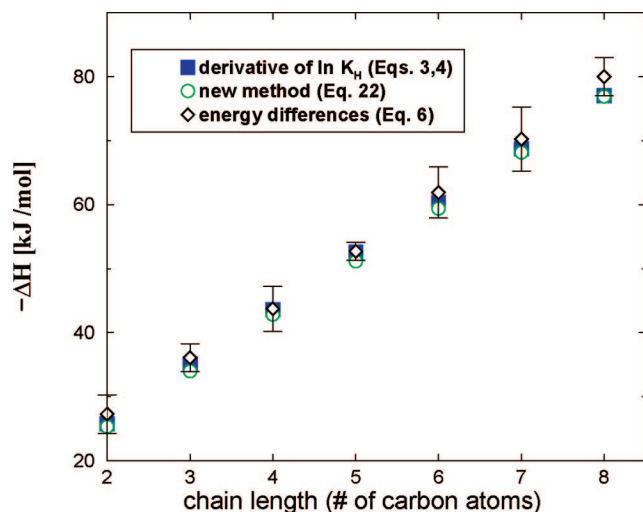


Figure 2. Heat of adsorption at zero loading for various n-alkanes in zeolite LTA5A computed using various methods. $T = 500$ K. We have included the error bars for the method based on energy differences. For the other two methods, we checked that the error bars are always smaller than the symbol size.

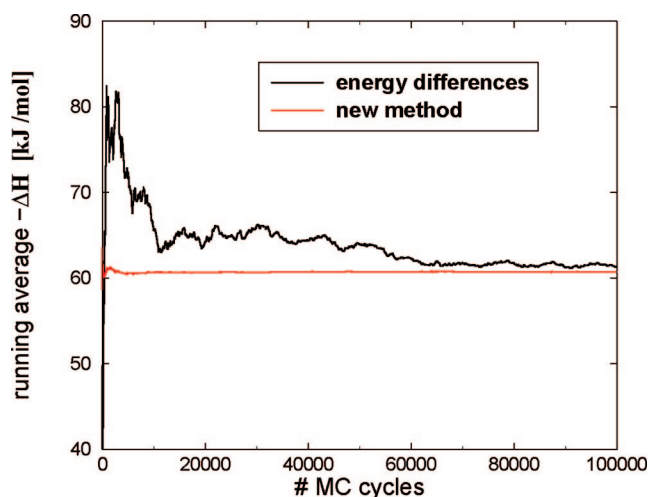


Figure 3. Running average of the heat of adsorption of n-hexane at zero loading as a function of the number of MC cycles for the method based on energy differences (eq 6) and our new method (eq 20). $T = 500$ K. Small displacements of the nonframework cations are allowed. Initial positions of the nonframework cations were taken from the crystallographic positions.³⁸

10^4 times smaller than either $\langle U_1 \rangle_1$ or $\langle U_0 \rangle_0$, and slightly smaller than the typical fluctuations of either $\langle U_1 \rangle_1$ or $\langle U_0 \rangle_0$, it is not surprising that the method based on energy differences performs poorly.

In all previous simulations (Figures 2 and 3), the initial positions of the nonframework cations were taken from the known crystallographic positions of LTA5A.³⁸ For this zeolite, also the positions of the framework Al atoms are well-known. Although the nonframework cations are allowed to move during the simulations, as expected their positions during the simulations do not significantly deviate from the crystallographic positions. However, in most cases, for a given zeolite the crystallographic positions of the nonframe-

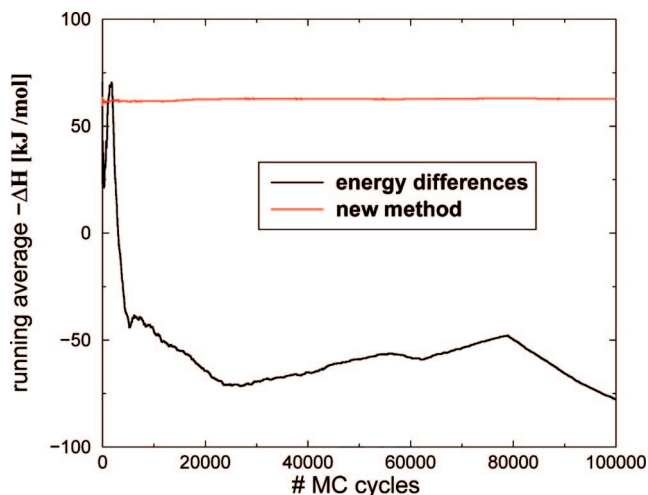


Figure 4. Running average of the heat of adsorption of n-hexane at zero loading as a function of the number of MC cycles for the method based on energy differences (eq 6) and our new method (eq 20), not starting from the crystallographic positions of the nonframework cations. $T = 500$ K. A simulation starting from random initial nonframework cation positions was conducted, and a long equilibration period was used. The final configuration of this simulation was used here as the starting point to compute the heat of adsorption. Trial moves to put nonframework cations at random positions in the zeolite are included to accelerate equilibration of the positions of the nonframework cations.

work cations or the framework Al atoms are not known from experiments. However, one could still be interested in computing the adsorption properties in this case. One should keep in mind that for some zeolites the adsorption properties strongly depend on the positions of the framework Al atoms, while for other zeolites this dependency is not present.^{19,20}

It is instructive to study this usual scenario further, i.e. the positions of the nonframework cations are not known. In this case, the only choice is to start from random initial positions of the nonframework cations and to use a long equilibration period of the system. Trial moves to put a nonframework cation at a random position in the zeolite will then significantly accelerate equilibration. It is important to note that this approach relies on the assumption that during the simulation the nonframework cations are able to find their equilibrium positions. This is a major cause for concern, as the interactions between the nonframework cations and the framework atoms are dominated by very strong electrostatic interactions, especially for multivalent ions like Ca.

To investigate the effect of possible rearrangements of the nonframework cations during the simulation, we conducted a simulation starting from random initial positions for the nonframework cations that was equilibrated for 10^5 cycles. Trial moves to put the nonframework cations at a random position in the zeolite were used to accelerate equilibration. The final configuration of the nonframework cations was then used as a starting point to compute the heat of adsorption using eqs 6 and 22, see Figure 4. Clearly, the method based on energy differences is extremely inaccurate as during the simulations the positions of the nonframework cations in the simulation with the n-hexane chain apparently deviate from

those in the simulation without the n-hexane chain, even though these simulations were started from the same initial nonframework cation positions. This difference in nonframework cation positions will have a huge effect on the total energies $\langle U_1 \rangle$ and $\langle U_0 \rangle$, and therefore it will dramatically affect the efficiency of any method to compute the heat of adsorption that requires more than one simulation of the host structure. In principle, the huge difference of Figure 4 would eventually disappear if one would simulate much longer, so that all rearrangements of nonframework cations would be visited according to their statistical weight. Unfortunately, due to the very strong interactions of the nonframework cations with the framework this will take extremely long simulations, even at high temperature (500 K).

From Figures 3 and 4 we can conclude that the method based on energy differences is very sensitive to the displacements of the nonframework cations and far less sensitive to the adsorption energy of a hydrocarbon. Therefore, the use of this method is not recommended for zeolites with strongly interacting nonframework cations. Note that the heat of adsorption of n-hexane calculated using our new method is approximately 60.7 kJ/mol for the simulations of Figure 3 and 62.7 kJ/mol for the simulations of Figure 4. As this difference is very small, one can conclude that the positions of the nonframework cations only have a minor influence on the heat of adsorption for LTA5A. However, performing the simulations with (arbitrary) fixed nonframework cation positions is not a sensible option as this may introduce other artifacts (especially when the temperature or loading is varied).¹⁷

5. Handling of Coulombic Interactions in Zeolites

In the previous section we have analyzed the difficulties introduced by strong electrostatic interactions in zeolites. Electrostatic interactions are very long-ranged due to their r^{-1} behavior. It is well-known that simple truncation of these interactions may lead to incorrect simulation results.^{14,39,40} Also, a direct summation of Coulombic pair interactions is conditionally convergent, i.e. the final result depends on the order of the summation. It is for this reason why the well-known Ewald summation^{41,26,14} or equivalent method is currently the generally accepted method in molecular simulations. For the Ewald summation, the total Coulombic energy of the system can be written as the sum of three contributions (assuming tin foil boundary conditions):

(1) The real-space part, which is proportional to

$$E_{\text{real}} = \sum_{i < j} \frac{q_i q_j \text{erfc}(\alpha r_{ij})}{r_{ij}} \quad (24)$$

in which $\text{erfc}(x)$ is the complementary error function, r_{ij} is the distance between particles i and j , q_i and q_j are the charges on particles i and j , respectively, and α is a constant damping factor. The summation $\sum_{i < j}$ is in principle a summation over all periodic images of i and j . However, it is convenient to choose α in such a way that only the nearest images have to be considered (as $\text{erfc}(x)$ is close to zero for large x). This requires a value of α that is not too small. The real-space

part of the Ewald summation and the conventional Lennard-Jones interactions can be calculated simultaneously using the same cutoff radius.

(2) The self-energy

$$E_{\text{self}} = -\frac{\alpha}{\sqrt{\pi}} \sum_{i=1}^N q_i^2 \quad (25)$$

which does not depend on the positions of the ions in the system.

(3) The Fourier part of the energy, which is proportional to

$$E_{\text{Fourier}} = \frac{1}{2V} \sum_{\mathbf{k} \neq 0} \frac{\exp[-k^2/4\alpha^2]}{k^2} \left| \sum_{j=1}^N q_j \exp[-i\mathbf{k} \cdot \mathbf{r}_j] \right|^2 \quad (26)$$

in which V is the volume of the system and the vectors \mathbf{k} are linear combinations of the reciprocal basis vectors of the system. For larger systems (>10000 charges), it is more efficient to replace eq 24 by a grid-based computation like Particle Mesh Ewald.¹⁴

The convergence of the total energy is controlled by the real-space cutoff r_{cut} , the value of α , and the number of vectors in each reciprocal direction (k). Provided that only nearest images are used to calculate the real-space energy (eq 22), the total energy as a function of the number of k -vectors converges to the same value for a large number of k -vectors, independent of the value of α (provided that α is sufficiently large).

The Fourier part of the system clearly depends on the positions \mathbf{r}_i (and charges q_i) of all N particles in the system. This may suggest that in a Monte Carlo simulation, in every trial move the positions of all particles in the system have to be considered for the calculation of the energy difference between the new and old configuration. Fortunately, it is possible to rewrite the Ewald summation in such a way that only the atoms with a different position have to be considered. The structure of eq 26 can be expressed as

$$E_{\text{Fourier}} \propto \sum_{\mathbf{k} \neq 0} |\mathbf{x}(\mathbf{k}, \mathbf{r}^N, \mathbf{q}^N)|^2 = \sum_{\mathbf{k} \neq 0} [\mathbf{R}(\mathbf{x}(\mathbf{k}))^2 + \mathbf{I}(\mathbf{x}(\mathbf{k}))^2] \quad (27)$$

in which the complex numbers x depends on the positions (\mathbf{r}^N) and charges (\mathbf{q}^N) of all the atoms in the system. The real and imaginary component of this vector can be expressed as

$$\mathbf{R}(\mathbf{x}(\mathbf{k})) = \sum_{i=1}^N q_i \cos(\mathbf{k} \cdot \mathbf{r}_i) \quad (28)$$

and

$$\mathbf{I}(\mathbf{x}(\mathbf{k})) = \sum_{i=1}^N q_i \sin(\mathbf{k} \cdot \mathbf{r}_i) \quad (29)$$

As $\mathbf{R}(\mathbf{x}(\mathbf{k}))$ and $\mathbf{I}(\mathbf{x}(\mathbf{k}))$ can be expressed as a summation over all particles in the system, it is convenient to store $\mathbf{R}(\mathbf{x}(\mathbf{k}))$ and $\mathbf{I}(\mathbf{x}(\mathbf{k}))$ in the memory of the computer (one complex number for each \mathbf{k}). For particle displacements, rotations, regrows, (test) insertions, deletions, and identity

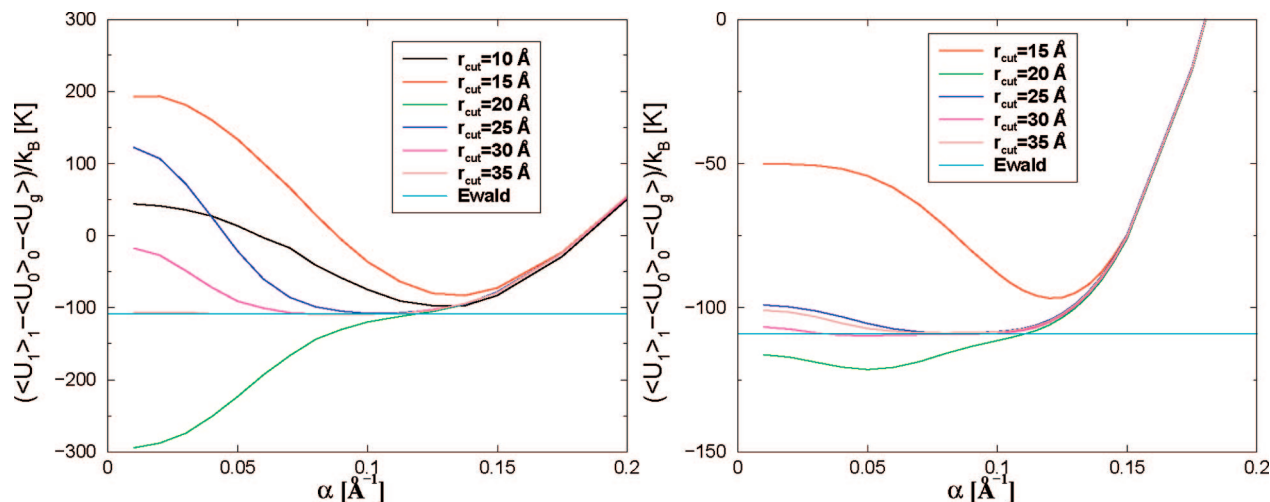


Figure 5. Average energy difference $\langle U_1 \rangle_1 - \langle U_0 \rangle_0 - \langle U_g \rangle$ for CO₂ in all silica MFI-type zeolite computed using the Wolf method (left) or using the modification by Fennell and Gezelter (right). The (unweighted) average is taken over all possible configurations of CO₂ that do not result in an overlap with zeolite atoms. The zeolite consists of $4 \times 4 \times 6$ unit cells. The size of the simulation box is therefore $a = 80.088 \text{ \AA}$, $b = 79.596 \text{ \AA}$, $c = 80.298 \text{ \AA}$. In all simulations, 3×10^7 trial insertions are used (eq 20). The result obtained by the Ewald summation ($\alpha = 0.3 \text{ \AA}^{-1}$, $k = 20$, $r_{\text{cut}} = 12 \text{ \AA}$) is also included.

changes one can easily calculate the new values for $\mathbf{R}(x(\mathbf{k}))$ and $\mathbf{I}(x(\mathbf{k}))$ by subtracting the contributions of the old configuration and adding the contributions for the new configuration. This has to be done only for atoms that have a different position in the old and new configuration.

Recently, Wolf and co-workers¹⁵ have proposed a pairwise alternative for the Ewald summation. In this method, the Coulombic interactions are damped using a complementary error function that is truncated and shifted at distance r_{cut} resulting in the following pair potential ($r_{ij} \leq r_{\text{cut}}$):

$$\varphi_{\text{Wolf}}(r_{ij}) = q_i q_j \left[\frac{\text{erfc}(\alpha r_{ij})}{r_{ij}} - \frac{\text{erfc}(\alpha r_{\text{cut}})}{r_{\text{cut}}} \right] \quad (30)$$

Fennell and Gezelter¹⁶ have developed a slightly modified damping function ($r_{ij} \leq r_{\text{cut}}$)

$$\varphi_{\text{FG}}(r_{ij}) = q_i q_j \left[\frac{\text{erfc}(\alpha r_{ij})}{r_{ij}} - \frac{\text{erfc}(\alpha r_{\text{cut}})}{r_{\text{cut}}} + (r_{ij} - r_{\text{cut}}) \left[\frac{\text{erfc}(\alpha r_{\text{cut}})}{r_{\text{cut}}^2} + \frac{2\alpha \exp[-\alpha^2 r_{\text{cut}}^2]}{\sqrt{\pi} r_{\text{cut}}} \right] \right] \quad (31)$$

Compared to the Ewald summation, the long-range Fourier part (eq 26) is omitted, which is only strictly correct in the limits $\alpha \rightarrow 0$ and $r_{\text{cut}} \rightarrow \infty$. To make a comparison between the results obtained from the Ewald summation and the Wolf method, one should not only consider the computational efficiency of the methods but also how the computed averages obtained from the methods depend on the control parameters (for the Wolf method, r_{cut} , α and for the Ewald summation r_{cut} , α and the number of k -vectors in each reciprocal direction (k)). As the cutoff radius is limited by the size of the simulation box (e.g., when the nearest image convention is used, r_{cut} is limited to half the boxsize¹⁴), a larger value of r_{cut} may imply that a zeolite consisting of more unit cells is required.

Although there have been several studies on the comparison between the Wolf method and the Ewald summation,^{16,42–44}

these studies mainly focus on reproducing the total energy of the simulation box at finite temperature and not on the energy change when a polar molecule is inserted into a simulation box. We have tested the Ewald summation and the Wolf method for calculating the heat of adsorption of CO₂ at zero loading in all silica MFI-type zeolite using the recently proposed force field of ref 45 (calculated using eq 22). As our goal is to investigate the differences between the Wolf method and the Ewald summation, we have eliminated all Lennard-Jones interactions, and all atoms in the system are modeled as hard spheres with a diameter of 3 Å. The partial charges of the atoms are taken as follows: $q_{\text{O(zeo)}} = -1.025e$, $q_{\text{Si(zeo)}} = +2.05e$, $q_{\text{C(CO}_2)} = +0.6512e$, $q_{\text{O(CO}_2)} = -0.3256e$. Grid interpolation techniques^{46,8} to compute pair potentials have not been used. As the self-interactions of the Wolf method for CO₂ and the zeolite are constant and independent of the reference state, only pair interactions between CO₂ and the zeolite (eqs 30 and 31) need to be considered for the Wolf method.

In Figure 5, we have plotted the energy difference $\langle U_1 \rangle_1 - \langle U_0 \rangle_0 - \langle U_g \rangle$ calculated using eq 22 for both the Wolf method and the modification by Fennell and Gezelter (eq 31) as a function of α for various values of the cutoff radius. In the same figure, the result obtained from the Ewald summation is also included. Clearly, the result strongly depends on the precise value of α and r_{cut} , especially for small values of r_{cut} . The value of $\alpha = 0.2 \text{ \AA}^{-1}$ as suggested by some authors^{16,43} leads to incorrect results for this system. At this point it is important to note that for practical usage of the Wolf method, the computed results should not depend too strongly on the precise values of r_{cut} and α . From Figure 5 it becomes clear that there is only a small range of α which leads to results consistent with the Ewald summation and that a cutoff radius of at least 25 Å is required to avoid a large sensitivity for the precise values of α and r_{cut} . This holds for both the original Wolf method and the modification by Fennell and Gezelter. Although for some values of α and

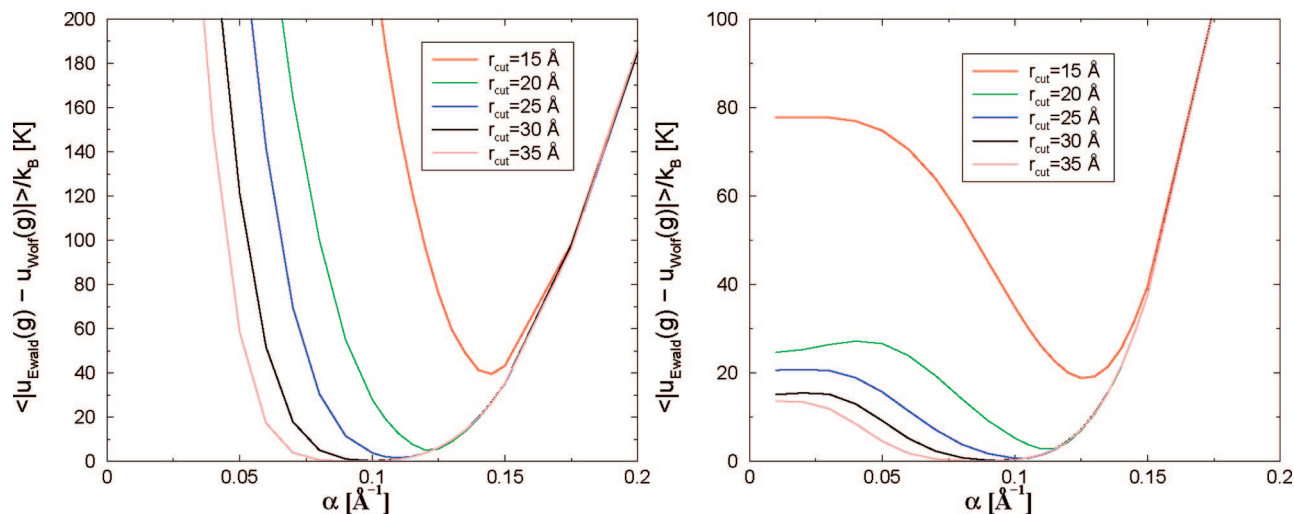


Figure 6. Absolute energy difference between the Ewald summation and the Wolf method for individual configurations of CO₂ (denoted as g) in MFI-type zeolite, averaged over all possible configurations of CO₂ that do not overlap with the zeolite. Left: Original Wolf method (eq 28). Right: The modification by Fennell and Gezelter (eq 29). The zeolite consists of $4 \times 4 \times 6$ unit cells. The size of the simulation box is therefore $a = 80.088$ Å, $b = 79.596$ Å, $c = 80.298$ Å. In all simulations, 3×10^7 trial insertions are used (eq 20).

r_{cut} the average heat of adsorption computed using the Wolf method is identical to the one computed using the Ewald summation, this does not guarantee that the energy of each individual configuration of CO₂ computed using both methods is identical. In Figure 6, we plotted the average absolute energy difference between the adsorption energy computed using the Ewald summation ($u_{\text{Ewald}}(g)$) and the adsorption energy computed using the Wolf method ($u_{\text{Wolf}}(g)$), calculated for the same configurations (g) of CO₂ and averaged over all possible configurations of CO₂ that do not overlap with the zeolite. For the optimal value of α for $r_{\text{cut}} = 20$ Å, the average absolute energy difference between the Wolf method and the Ewald summation for a single configuration of CO₂ is on average 4%, while the difference in average energy is zero for the optimal value of α . This means that although the Wolf method may predict correct averages for the optimal α and r_{cut} , one should also test whether the energy of individual configurations is computed correctly (i.e., identical to the result obtained by the Ewald summation). If this is not the case, one can expect artifacts in the simulation results. From Figures 5 and 6 it becomes clear that the Wolf method only converges to the correct energy for each configuration of CO₂ for (1) a cutoff radius of at least 25 Å and (2) a narrow range of α .

The results of the Ewald summation are not very sensitive to the precise values of α and r_{cut} , see Table 1. It is well-known that if only nearest images are used to compute the real-space part of the energy (eq 24), the total energy of the system as a function of k at constant α should always converge to the same value for large k , provided that α is large enough. The difference between the averages in Table 1 is less than 1% which is approximately equal the error in any of the reported values in Table 1. We verified that the energy of each single configuration of CO₂ is within 0.1% for any of the values of α , r_{cut} , and k reported in Table 1. It is important to note that the finite-size effect is absent for our system when charges are handled using the Ewald summation, and therefore one can use a small simulation

Table 1. Average Energy Difference $\langle U_1 \rangle_1 - \langle U_0 \rangle_0 - \langle U_g \rangle$ for CO₂ in All Silica MFI-Type Zeolite Computed Using the Ewald Summation^a

no. of unit cells	α [Å ⁻¹]	k	r_{cut} [Å]	$(\langle U_1 \rangle_1 - \langle U_0 \rangle_0 - \langle U_g \rangle)/k_B$ [K]
$4 \times 4 \times 6$	0.4	30	20	-110.4
$2 \times 2 \times 3$	0.3	15	12	-108.9
$2 \times 2 \times 3$	0.3	20	12	-109.8
$2 \times 2 \times 3$	0.3	30	12	-109.6
$2 \times 2 \times 3$	0.4	10	12	-110.6
$2 \times 2 \times 3$	0.4	20	12	-110.1
$2 \times 2 \times 3$	0.3	10	18	-109.2
$2 \times 2 \times 3$	0.3	20	18	-109.2
$2 \times 2 \times 3$	0.3	30	18	-109.2
$2 \times 2 \times 3$	0.5	20	18	-109.6

^a In all simulations, 3×10^7 trial insertions are used (eq 22).

box ($2 \times 2 \times 3$ unit cells). For the Wolf method however, this is not possible as a cutoff radius of at least 25 Å is needed. According to the nearest image convention the size of the simulation box needs to be at least twice the value of r_{cut} . Using such a large cutoff radius is inconvenient, as the usual sorbate-zeolite and sorbate-sorbate Lennard-Jones type interactions have a cutoff radius of typically 12 Å.^{11,12,17,47} We compared the CPU time required for the Wolf method for $\alpha = 0.1$ Å⁻¹ and $r_{\text{cut}} = 25$ Å ($4 \times 4 \times 6$ unit cells) with the Ewald summation ($\alpha = 0.3$ Å⁻¹, $k = 15$, $r_{\text{cut}} = 12$ Å, $2 \times 2 \times 3$ unit cells) for the same number of trial insertions of CO₂. Although in this simulation using the Ewald method 88% of the CPU time is spent in calculating the Fourier energy (eq 24), the simulation using the Ewald method is still 7 times faster due to the fact that a smaller cutoff radius can be used.

While other studies found quite good agreement between the Wolf method and the Ewald summation for condensed phases,^{16,42-44} our findings (Figures 5 and 6) show that convergence to the Ewald result is more difficult for zeolites. The reason is that the Wolf method critically depends on the screening of electrostatics around a central ion. Due to the screening the effective range of the potential will be

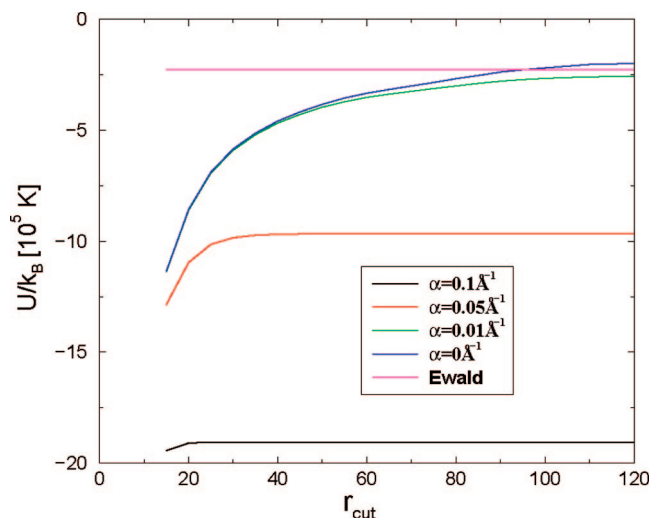


Figure 7. Total energy of a single configuration of 100 randomly placed Na^+ ions and 100 randomly placed Cl^- ions in a simulation box of $250 \text{ Å} \times 250 \text{ Å} \times 250 \text{ Å}$, computed using the Ewald summation, the Wolf method, and a direct r^{-1} summation ($\alpha = 0 \text{ Å}^{-1}$). Hard-core overlaps are avoided in this single configuration.

reduced, and therefore a summation of pair interactions seems sufficient to describe effective interactions between ions. As a large part of the zeolite consists of empty pores (at low loading), the screening of Coulombic interactions is less efficient and a large cutoff radius is required.

It is instructive to test the convergence of the Wolf method for a worse-case scenario, i.e. a system that is highly disordered with large concentration gradients, even though the Wolf method was not designed for such a system. For molten NaCl at high density, it has been shown that the total energy computed by the Wolf method is in reasonable agreement with the Ewald summation.⁴⁴ Consider a system of 100 Na^+ ions and 100 Cl^- ions in a simulation box of $250 \text{ Å} \times 250 \text{ Å} \times 250 \text{ Å}$, the density of this system is extremely low. The ions are placed at random positions in the simulation box in such a way that hard-core overlaps (here: ion–ion distance smaller than 3 Å) are avoided. For a single configuration of the ions, we investigated the total energy computed using the Wolf method for various values of α ¹⁵

$$E_{\text{Wolf}} = -\left(\frac{\alpha}{\sqrt{\pi}} + \frac{\text{erfc}(\alpha r_{\text{cut}})}{2r_{\text{cut}}}\right) \sum_{i=1}^N q_i^2 + \sum_{i < j} \varphi_{\text{Wolf}}(r_{ij}) \quad (32)$$

The results are shown in Figure 7. Clearly, for $\alpha = 0.1 \text{ Å}^{-1}$ and $\alpha = 0.05 \text{ Å}^{-1}$ the total energy of the Wolf method converges to an incorrect total energy. For $\alpha = 0.01 \text{ Å}^{-1}$, the energy of the Wolf method converges to the result obtained by the Ewald summation. However, the convergence is just as slow as a direct r^{-1} summation of pair interactions ($\alpha = 0 \text{ Å}^{-1}$ in eq 28). This clearly shows that the Wolf method critically depends on the screening of electrostatic interactions and that for a given system one should always check whether such a screening is applicable.

It is well-known that a direct r^{-1} summation only converges for very large values of the cutoff radius,¹⁴ for example more than 40 Å for neutral molecules. Damping the Coulombic potential reduces this range, although still a

cutoff of at least 25 Å seems to be the minimum requirement, but at the cost of uncertainty in the damping constant α . Different values for α are recommended in the literature implying this damping is system specific and possibly dependent on the molecule type, framework topology, temperature, etc. The Ewald summation is able to compute the electrostatic energy exactly (to within any specified numerical precision) for a system of charges in an infinitely periodic structure at a cost less than quadratic with the number of particles ($N^{3/2}$ for Ewald). The energy and forces computed with the Ewald summation are well-defined and unique. They do not depend on a judicious choice of damping parameters and cutoff values, and Ewald type methods are at the same level of accuracy significantly cheaper.

6. Conclusions

We have introduced a new method to compute the heat of adsorption for adsorbates in framework structures with nonframework cations that requires only a single simulation of the host. The main difference with the conventional Widom's test particle method is that Widom's test particle method only provides the Henry coefficient at a certain temperature, and therefore, additional simulations at different temperatures and a numerical differentiation will be necessary to compute the heat of adsorption. The often used method based on energy differences is far more sensitive to the precise displacements of the nonframework cations than to the interactions with the adsorbate and therefore this method is unsuited for structures with nonframework cations. In addition, we have shown that for studying adsorption in zeolites, the Ewald summation is superior to the recently proposed Wolf method (and other direct summation methods), both in accuracy and speed. The Ewald method can be implemented very efficiently for Monte Carlo methods as only the change for moving atoms needs to be computed.

Acknowledgment. T.J.H.V. acknowledges The Netherlands Organization for Scientific Research (NWO-CW) for financial support through a VIDI grant. This work is supported by the Spanish "Ministerio de Educación y Ciencia" (CTQ2007-63229/BQU) and by the resources, technical expertise, and assistance provided by BSC-CNS, and by the National Science Foundation (CTS-0507013).

Appendix: Chemical Potential

The chemical potential of a chain molecule can be computed using the Rosenbluth scheme³⁶

$$\beta\mu = -\ln\langle W \rangle \quad (33)$$

in which W is the Rosenbluth weight. Consider the situation that we use f trial positions for the first bead and k trial positions for the other $N-1$ beads. The Rosenbluth weight W is then defined as

$$W = \frac{\prod_{i=1}^N \sum_j \exp[-\beta u_{ij}]}{f k^{N-1}} \quad (34)$$

in which u_{ij} is the energy of the j th trial position of the i th

chain segment. In this scheme, trial directions are selected with a probability

$$P_{\text{sel}} = \frac{\exp[-\beta u_{ij}]}{\sum_j \exp[-\beta u_{ij}]} \quad (35)$$

It is sometimes convenient to choose a different selection of trial segments than in the Rosenbluth scheme,

$$P_{\text{sel}}^* = \frac{\exp[-\beta u_{ij}^*]}{\sum_j \exp[-\beta u_{ij}^*]} \quad (36)$$

in which $u_{ij}^* \neq u_{ij}$. This is for example useful for charged systems, in which only the real-space part of the Coulombic potential is used to select trial segments. Another application is the use of a second cutoff radius to select trial segments.^{27,37}

Below, we will show that in the case of a different selection rule for trial segments, the chemical potential can be computed using

$$\beta\mu = -\ln\langle W \rangle = -\ln \left\langle \frac{\prod_{i=1}^N \sum_j \exp[-\beta u_{ij}^*]}{j k^{N-1}} \times \exp[-\beta\delta] \right\rangle = -\ln\langle W^* \times \exp[-\beta\delta] \rangle \quad (37)$$

in which δ is the energy difference $\delta = \sum_i [u_{ij(i)} - u_{ij(i)}^*]$ in which $j(i)$ is the selected trial direction for segment i . Note that if $u_{ij}^* = u_{ij}$, then we recover eq 36, and if $u_{ij}^* = 0$, then we have $W^* = 1$ and we recover the original Widom's test particle method.¹⁴ To show that eq 37 is correct, consider the extension of a chain with a single trial segment. The probability of generating a given set of k trial directions with orientations $\mathbf{\Gamma}_1$ though $\mathbf{\Gamma}_k$ is

$$P_{\text{gen}}(\mathbf{\Gamma}_1) \cdots P_{\text{gen}}(\mathbf{\Gamma}_k) d\mathbf{\Gamma}_1 \cdots d\mathbf{\Gamma}_k \quad (38)$$

The probability to select any of these trial segment follows from eq 36:

$$P_{\text{sel}}^* = \frac{\exp[-\beta u_{ij}^*]}{\sum_j \exp[-\beta u_{ij}^*]} = \frac{\exp[-\beta u_{ij}^*]}{w_i^*(\mathbf{\Gamma}_1 \cdots \mathbf{\Gamma}_k)} \quad (39)$$

We have to consider the average of $w_i^* \exp[-\beta(u_{ij} - u_{ij}^*)]$ over all possible sets of trial segments (j) and all possible choices of the trial segment (j'):

$$\begin{aligned} & \left\langle \frac{w_i^* \exp[-\beta(u_{ij} - u_{ij}^*)]}{k} \right\rangle \\ &= \int \prod_{j=1}^k d\mathbf{\Gamma}_j P_{\text{gen}}(\mathbf{\Gamma}_j) \sum_{j'=1}^k P_{\text{sel}}^* \times \frac{w_i^* \exp[-\beta(u_{ij} - u_{ij}^*)]}{k} \\ &= \int \prod_{j=1}^k d\mathbf{\Gamma}_j P_{\text{gen}}(\mathbf{\Gamma}_j) \sum_{j'=1}^k \frac{\exp[-\beta u_{ij}^*]}{w_i^*} \times \frac{w_i^* \exp[-\beta(u_{ij} - u_{ij}^*)]}{k} \\ &= \int \prod_{j=1}^k d\mathbf{\Gamma}_j P_{\text{gen}}(\mathbf{\Gamma}_j) \sum_{j'=1}^k \frac{\exp[-\beta u_{ij}]}{k} \end{aligned} \quad (40)$$

As the labeling of trial segment is arbitrary, this leads to

$$\left\langle \frac{w_i^* \exp[-\beta(u_{ij} - u_{ij}^*)]}{k} \right\rangle = \int d\mathbf{\Gamma} P_{\text{gen}}(\mathbf{\Gamma}) \exp[-\beta u_i] \quad (41)$$

By definition, we have¹⁴

$$\left\langle \frac{w_i}{k} \right\rangle = \int d\mathbf{\Gamma} P_{\text{gen}}(\mathbf{\Gamma}) \exp[-\beta u_i] \quad (42)$$

in which

$$w_i = \sum_{j=1}^k \exp[-\beta u_{ij}] \quad (43)$$

This proves that

$$\langle W \rangle = \langle W^* \exp[-\beta\delta] \rangle \quad (44)$$

In a similar way, one can show that

$$\langle F \times W \rangle = \langle F \times W^* \exp[-\beta\delta] \rangle \quad (45)$$

in which F can be an arbitrary function that only depends on the position of the generated chain.

References

- (1) Baerlocher, Ch.; McCusker, L. B.; Olson, D. H. *Atlas of Zeolite Framework Types*, 6th ed.; Elsevier: Amsterdam, 2007.
- (2) Bezus, A. G.; Kiselev, A. V.; Lopatkin, A. A.; Du, P. Q. *J. Chem. Soc., Faraday Trans. II* **1978**, 74, 367.
- (3) Snurr, R. Q.; Bell, A. T.; Theodorou, D. R. *J. Phys. Chem.* **1993**, 97, 13742.
- (4) Smit, B.; Siepmann, J. I. *Science* **1994**, 264, 1118.
- (5) Smit, B.; Maesen, Th. L. M. *Nature* **1995**, 374, 42.
- (6) Maginn, E. J.; Bell, A. T.; Theodorou, D. N. *J. Phys. Chem.* **1995**, 99, 2057.
- (7) Macedonia, M. D.; Maginn, E. J. *Mol. Phys.* **1999**, 96, 1375.
- (8) Vlugt, T. J. H.; Krishna, R.; Smit, B. *J. Phys. Chem. B* **1999**, 103, 1102.
- (9) Fuchs, A. H.; Cheetham, A. K. *J. Phys. Chem. B* **2001**, 105, 7375.
- (10) Pascual, P.; Ungerer, P.; Tavittian, B.; Pernot, P.; Boutin, A. *Phys. Chem. Chem. Phys.* **2003**, 5, 3684.
- (11) Dubbeldam, D.; Calero, S.; Vlugt, T. J. H.; Krishna, R.; Maesen, Th. L. M.; Smit, B. *J. Phys. Chem. B* **2004**, 108, 12301.
- (12) Dubbeldam, D.; Calero, S.; Vlugt, T. J. H.; Krishna, R.; Maesen, Th. L. M.; Beerdse, E.; Smit, B. *Phys. Rev. Lett.* **2004**, 93, 088302.
- (13) Liu, B.; Smit, B.; Calero, S. *J. Phys. Chem. B* **2006**, 110, 20166.
- (14) Frenkel, D.; Smit, B. *Understanding Molecular Simulation: from Algorithms to Applications*, 2nd ed.; Academic Press: San Diego, CA, 2002.
- (15) Wolf, D.; Keblinski, P.; Phillpot, S. R.; Eggebrecht, J. *J. Chem. Phys.* **1999**, 110, 8254.
- (16) Fennell, C. J.; Gezelter, J. D. *J. Chem. Phys.* **2006**, 124, 234104.
- (17) Calero, S.; Dubbeldam, D.; Krishna, R.; Smit, B.; Vlugt, T. J. H.; Denayer, J. F. M.; Martens, J. A.; Maesen, Th. L. M.

- J. Am. Chem. Soc.* **2004**, 126, 11377.
- (18) García-Pérez, E.; Dubbeldam, D.; Maesen, Th. L. M.; Calero, S. *J. Phys. Chem. B* **2006**, 110, 23968.
- (19) García-Pérez, E.; Dubbeldam, D.; Liu, B.; Smit, B.; Calero, S. *Angew. Chem.* **2006**, 45, 276.
- (20) Liu, B.; García-Pérez, E.; Dubbeldam, D.; Smit, B.; Calero, S. *J. Phys. Chem. C* **2007**, 111, 10419.
- (21) Wood, G. B.; Panagiotopoulos, A. Z.; Rowlinson, J. S. *Mol. Phys.* **1988**, 63, 49.
- (22) Dunne, J. A.; Mariwala, R.; Rao, M.; Sircar, S.; Gorte, R. J.; Myers, A. L. *Langmuir* **1996**, 12, 5888.
- (23) Smit, B.; Siepmann, J. I. *J. Phys. Chem.* **1994**, 98, 8442.
- (24) Karavias, F.; Myers, A. L. *Langmuir* **1991**, 7, 3118.
- (25) Widom, B. *J. Chem. Phys.* **1963**, 39, 2802.
- (26) Allen, M. P.; Tildesley, D. J. *Computer Simulation of Liquids*; Clarendon Press: Oxford, 1987.
- (27) Vlugt, T. J. H. *Mol. Simul.* **1999**, 23, 63.
- (28) Siepmann, J. I.; Frenkel, D. *Mol. Phys.* **1992**, 75, 59.
- (29) Frenkel, D.; Mooij, G. C. A. M.; Smit, B. *J. Phys.: Condens. Matter* **1992**, 4, 3053.
- (30) de Pablo, J. J.; Laso, M.; Suter, U. W. *J. Chem. Phys.* **1992**, 96, 6157.
- (31) Siepmann, J. I. In *Computer simulation of biomolecular systems: theoretical and experimental applications*; van Gunsteren, W. F., Weiner, P. K., Wilkinson, A. J., Eds.; Escom Science Publisher: Leiden, 1993; p 249.
- (32) Press, W. H.; Flannery, B. P.; Teukolsky, S. A.; Vetterling, W. T. *Numerical Recipes: The art of scientific computing*; Cambridge University Press: Cambridge, 1986.
- (33) Consta, S.; Wilding, N. B.; Frenkel, D.; Alexandrowicz, Z. *J. Chem. Phys.* **1999**, 110, 3220.
- (34) Consta, S.; Vlugt, T. J. H.; Wichers Hoeth, J.; Smit, B.; Frenkel, D. *Mol. Phys.* **1999**, 97, 1243.
- (35) Combe, N.; Vlugt, T. J. H.; ten Wolde, P. R.; Frenkel, D. *Mol. Phys.* **2003**, 101, 1675.
- (36) Rosenbluth, M. N.; Rosenbluth, A. W. *J. Chem. Phys.* **1955**, 23, 356.
- (37) Vlugt, T. J. H.; Martin, M. G.; Smit, B.; Siepmann, J. I.; Krishna, R. *Mol. Phys.* **1998**, 94, 727.
- (38) Pluth, J. J.; Smith, J. V. *J. Am. Chem. Soc.* **1980**, 102, 4704.
- (39) Patra, M.; Karttunen, M.; Hyvönen, M. T.; Falck, E.; Lindqvist, P.; Vattulainen, I. *Biophys. J.* **2003**, 84, 3636.
- (40) Patra, M.; Karttunen, M.; Hyvönen, M. T.; Falck, E.; Vattulainen, I. *J. Phys. Chem. B* **2004**, 108, 4485.
- (41) Ewald, P. P. *Ann. Phys.* **1921**, 64, 253.
- (42) Demontis, P.; Spanu, S.; Suffritti, G. B. *J. Chem. Phys.* **2001**, 114, 7980.
- (43) Zahn, D.; Schilling, B.; Kast, S. M. *J. Phys. Chem. B* **2002**, 106, 10725.
- (44) Avendano, C.; Gil-Villegas, A. *Mol. Phys.* **2006**, 104, 1475.
- (45) García-Pérez, E.; Parra, J. B.; Ania, C. O.; García-Sánchez, A.; van Baten, J. M.; Krishna, R.; Dubbeldam, D.; Calero, S. *Adsorption* **2007**, 13, 469.
- (46) June, R. L.; Bell, A. T.; Theodorou, D. N. *J. Phys. Chem.* **1992**, 96, 1051.
- (47) Martin, M. G.; Thompson, A. P.; Nenoff, T. N. *J. Chem. Phys.* **2001**, 114, 7174.

CT700342K